УДК 621.455:519.876.5

I. LEVCHENKO[1], M. ROMANOV[1], A. VOLOSHKO[2], S. GULYI[1]

[1]*National Aerospace University, Kharkov, Ukraine*
[2]*ISMA NTK "Institute of monocrystals", National Academy of Sciences of Ukraine*

MOVEMENT OF UNIPOLAR ARCS IN MAGNETIC FIELD

In this paper we present the results of experimental investigation of the unipolar arc movement in a magnetic field, and a model and results of numerical simulation of the unipolar arc ignition process. We have found that on the ignition stage the unipolar arc is very sensitive to the plasma parameters and may be extinguished due to small variation of the plasma density and electron temperature. The arc behavior is determined mainly by the electron energy and plasma density. The essential current surges are possible due to the plasma – wall capacitance.

unipolar arc, magnetic field

Introduction

Unipolar arcs are specific breakdowns that take place between a bulk plasma and surface of the biased electrode, and cause an intense mass transfer between the plasma and electrode. Some experimental effects caused by the unipolar arc interaction with the electrodes were described somewhere [1, 2]. The unipolar arc models usually consider the formation of a sheath between plasma and an electrode surface contacting with the plasma. The electrons have high thermal velocity relative to the ion velocity, and hence the high-energy electrons in the distribution function are lost from the plasma to the wall, and the plasma assumes a positive potential relative to the wall [3]. If plasma sheath potential is sufficient to ignite and sustain an arc, a unipolar arc can occur. The breakdown takes place when the voltage drop between the plasma and cathode exceeds the arc potential drop (about the metal ionization potential), or when the field emission caused by the electrical field on the roughness peaks reaches the value required for the breakdown. After the initial ignition, the explosive heating provides the hot spot formation and the further arcing process.

The unipolar arc is extinguished die to the hot spot collapse, as a result of molten metal ejection followed by the abrupt cooling the emitting area, or in case of the plasma sheath depletion.

1. Experimental Setup

A scheme of the experiment is shown in fig. 1.

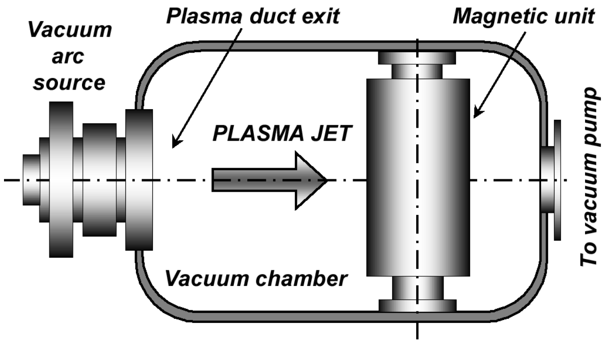

Fig. 1. Scheme of the experiment with cylindrical probe

The equipment consists of a stainless steel vacuum chamber, a gas pumping system, a gas supply system, a vacuum arc plasma source, and two probes (spherical and cylindrical) mounted on the insulating supports. The chamber walls were grounded. The vacuum arc plasma source incorporates a cathode of 60 mm diam. and a stainless steel anode of 100 mm dia. The plasma source current is 100 A at nominal voltage of 80 V. The source operates in a steady-state regime, and the ignition is achieved by the automatic system with the use of a special ignitor. The vacuum system consists of an oil vapor diffusion pump, a mechanical backing pump and a gas supply electromagnetic valve that was capable of maintaining a nitrogen pressure in the range of 0,1 to

1 Pa. The pressure was measured with a thermocouple vacuum gauge and an ionization gauge. The cylindrical probe (fig. 2) was made from non-magnetic stainless steel tube of 145 mm diam.

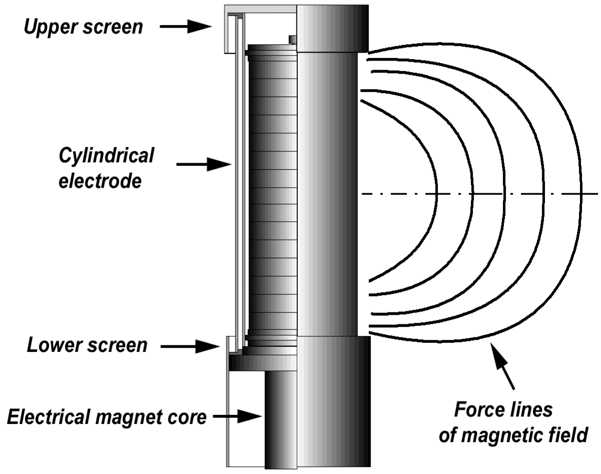

Fig. 2. Scheme of the cylindrical probe

The magnetic coil of 95 mm diam. and 125 mm long was installed inside the tube. The spherical probe (fig. 3) of 145 mm diam. was made of non-magnetic stainless steel of 1 mm thick. Between two hemispheres the magnetic core of 45 mm diam. was installed, on which the magnetic coil of 95 mm diam. and 115 mm long was installed. The coil was wound with a copper wire of 0,8 mm diam. The magnetic field strength was controlled by changing the coil current in the range of 2 to 10 A. The maximum magnetic field strength on the probe surface reaches 0.05 T for coil current I_m = 10 A. The magnetic field configurations are shown in fig. 2 and fig. 3. The probes were biased with voltage of 0 to –1000 V. The voltage, current, and pressure were measured with electronic measuring instruments. The nature of UA traces in the central (fig. 4, a) and upper (fig. 4, b) zones of the electrodes is different. The traces in the upper zone have a typical "crow's foot" shape. The traces in the central zone are the tracks that branch off the common "stem" located in the upper part of the damaged area.

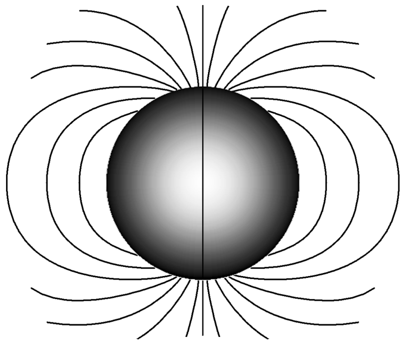

Fig. 3. Scheme of the spherical probe

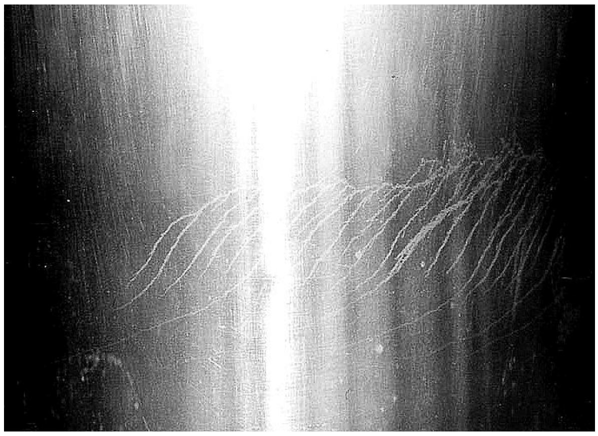

a

b

Fig. 4. Traces of unipolar arcs:
a – in central zone of the cylindrical electrode; direction of arc motion – R to L; b – in upper zone of the cylindrical electrode; direction of arc motion – L to R

2. Model

For modeling the initial stage of the unipolar arc ignition, the following system of equation was used.

Initial cathode potential

$$U_C = \frac{W_0}{2}\ln\left(\frac{m_i}{m_e}\right), \qquad (1)$$

where W_0 – plasma electron energy, eV, m_i is the ion mass, and m_e is the electron mass.

The initial discharge is due to the plasma – cathode capacity discharge with the characteristic time being of t_o (unipolar arc origination characteristic time); so, the minimum resistance can be calculated as:

$$R_{MIN} = \frac{U_M}{J_M} = \frac{U_M}{Q/t_0} = \frac{U_M t_0}{CU_C} = k_U\frac{t_0}{C}, \qquad (2)$$

where U_M is mean discharge potential; J_M is mean discharge current; C is the plasma – cathode capacity, and $k_U \approx 0{,}2 \ldots 0{,}1$.

There are two possible ways for choosing the characteristic time t_o. Firstly, the t_o value can be determined as a time of the 'usual' cathode arc ($10^{-8} \ldots 10^{-9}$ s); secondly, the t_o value can be evaluated from the fact that the minimum unipolar arc traces are the craters of 1 … 3 μm. With the cathode potential and characteristic current known from the experiment, the minimum time required can be calculated. This estimation provides $t_o = 10^{-8} \ldots 10^{-9}$ s as well.

The plasma – cathode spot resistance was calculated in the assumption that the resistance decreases to the R_{MIN} value and then increases to the initial value during the time required for crater formation (2 to 3 μm on the steel). The crater formation was calculated on the base of the metal heating and melting, in the assumption that the main molted mass was splashed out. So we assumed:

$$R(t) = R_0 \cdot \left(1 - \exp^{-\lambda(t-t_0)^2}\right) + R_{MIN}, \qquad (3)$$

where the factor λ was calculated from the above assumptions.

The discharge current was consequently calculated:

$$J_D(t) = \frac{U_C(t)}{R(t)}. \qquad (4)$$

The plasma electron current to the cathode cab be calculated by integrating electron distribution function:

$$J_P(t) = S_C \int_{U_C(t)}^{\infty} f(\varepsilon)\cdot d\varepsilon, \qquad (5)$$

where $f(\varepsilon)$ ids the electron distribution function (Maxwell distribution in this case), S_C is the cathode area, ε is the electron energy, and $U_C(t)$ is the cathode potential.

The cathode charge and potential were calculated:

$$Q_C(t) = \int_0^t (J_P - J_D)d\tau; \quad U_C(t) = \frac{Q_C(t)}{C}, \qquad (6)$$

where τ is the time.

The discharge energy was calculated:

$$\varepsilon_D = \int_0^{\infty} J(t)U_C(t)dt. \qquad (7)$$

The plasma current energy was calculated:

$$\varepsilon_P = S_C U_C(t) \int_{U_C(t)}^{\infty} f(\varepsilon)\cdot d\varepsilon. \qquad (8)$$

3. Results

The system was solved numerically for the following initial conditions:

1) plasma electron mean energy: $W_0 = 1 \ldots 5$ eV;
2) electron concentration: $n = 1\cdot10^{17} \ldots 5\cdot10^{17}$ m^{-3};
3) $s_c = 10$ cm^2;
4) C = 20 … 100 pF;
5) $t_0 = 10^{-9} \ldots 10^{-8}$ s.

The dependencies of the discharge current (upper curve) and plasma electron current (lower curve) are shown below (see fig. 5). The discharge energy corresponds to the crater formation of 2 μm on the Fe. It can be seen that under these conditions the unsteady process is present. The plasma current pulse has a phase lag relative to the discharge current. The maximum current values are different. The crater is mainly formed due to the capacity discharge followed by the charging with plasma current.

With the arcing time increased, the situation is appreciably changed. The stationary area with discharge current J_D equal to the plasma current J_P arrears, and the

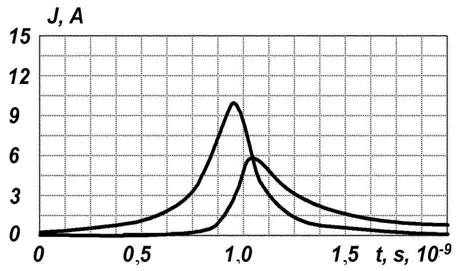

Fig. 5. Dependencies of the discharge current (upper curve) and plasma electron current (lower curve)

discharge energy increases. This case corresponds to the large crater formation. This situation is illustrated in fig. 6. In this model the Maxwell electron distribution was used for the charging process calculation; this causes the slow charging rate with the cathode potential approaching the maximum possible value.

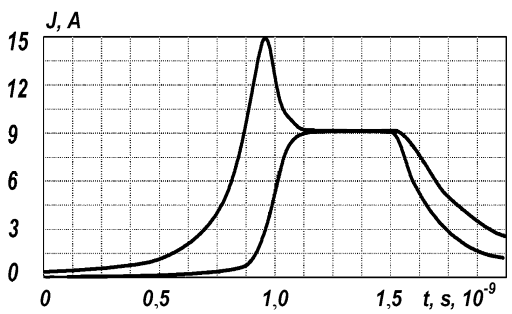

Fig. 6. Dependencies of the cathode potential on time

It is apparent that with the stationary zone increasing the influence of transient zone decreases. This case corresponds to the big crater; in the stationary mode $J_D = J_P$. After the discharge interruption, the second transient process takes place with the plasma current exceeding the discharge current (for each time moment). The first stage of the arc ignition was modeled in details using the above set of equations. It was found that on the first stage of burning the unipolar arc is very sensitive to the plasma parameters. The current – time curves for the stage of a spot formation are shown in fig. 7. The curves 4 and 5 correspond to the stable spot formation; curves 1, 2, and 3 correspond to the extinguishing process caused by small variation of the plasma parameters. The point of curves bifurcation corresponds to the melted metal splash.

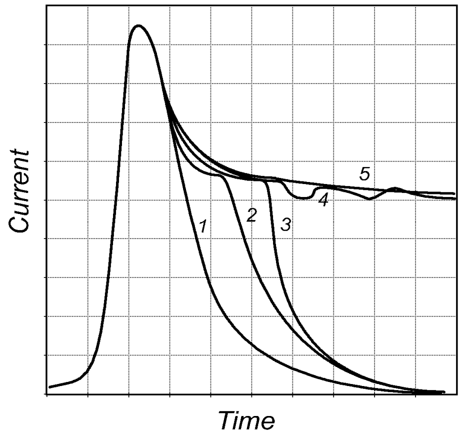

Fig. 7. Current – time curves for stage of spot formation

Conclusions

In this paper we have presented a model and results of numerical simulation of the unipolar arc ignition process. We have found that on the ignition stage the unipolar arc is very sensitive to the plasma parameters. The arc behavior is determined mainly by the electron energy and plasma density. The essential current surges are possible due to the plasma – wall capacitance. These features can explain the high-frequency arc cutoff phenomena found in the experiments.

References

1. Schwirzke F.R., Hallal M.P., Maruyama X.K. Onset of breakdown and formation of cathode spots // IEEE Trans. Plasma Sci. – 1993. – Vol. 21, No. 5. – P. 410 – 415.

2. Gielen H. J.G., Schram D.C. Unipolar arc model // IEEE Trans. Plasma Sci. – 1990. – Vol. 18, No. 1. – P. 127 – 133.

3. Schwirzke F.R. Vacuum breakdown on metal surfaces // IEEE Trans. Plasma Sci. – 1990. – Vol. 19, No. 5. P. 690 – 696.

Поступила в редакцию 02.11.2004

Рецензент: канд. техн. наук В.И. Маляковский, Национальный аэрокосмический университет им. Н.Е. Жуковского «ХАИ», Харьков.